CERN-ACC-2014-0294

HiLumi LHC

FP7 High Luminosity Large Hadron Collider Design Study

Deliverable Report

Issues In Special Magnets Studies

Fessia, Paolo (CERN) *et al*

28 November 2014

The HiLumi LHC Design Study is included in the High Luminosity LHC project and is partly funded by the European Commission within the Framework Programme 7 Capacities Specific Programme, Grant Agreement 284404.

This work is part of HiLumi LHC Work Package **3: Magnets for Insertion Regions**.

The electronic version of this HiLumi LHC Publication is available via the HiLumi LHC web site <http://hilumilhc.web.cern.ch> or on the CERN Document Server at the following URL: <http://cds.cern.ch/search?p=CERN-ACC-2014-0294>

CERN-ACC-2014-0294

Grant Agreement No: 284404

HILUMI LHC

FP7 High Luminosity Large Hadron Collider Design Study

Seventh Framework Programme, Capacities Specific Programme, Research Infrastructures, Collaborative Project, Design Study

DELIVERABLE REPORT

ISSUES IN SPECIAL MAGNETS STUDIES

DELIVERABLE: D3.1

Document identifier:	HILUMILHC-Del-D3-1-v1.0
Due date of deliverable:	End of Month 36 (October 2014)
Report release date:	28/11/2014
Work package:	WP3 IR Magnets
Lead beneficiary:	CEA
Document status:	Final

Abstract:

The HiLumi LHC Design Study is included in the High Luminosity LHC project and is partly funded by the European Commission within the Framework Programme 7 Capacities Specific Programme, Grant Agreement 284404. HiLumi LHC began in November 2011 and will run for 4 years.

Delivery Slip

	Name	Partner	Date
Authored by	P. Fessia, G. Kirby, E. Todesco M. Segreti, J. M. Rifflet	CERN CEA	06/11/2014
Edited by	C. Noels	CERN	06/11/2014
Reviewed by	L. Rossi, Project Coordinator	CERN	10/11/2014
Approved by	Steering Committee		17/11/2014

TABLE OF CONTENTS

Executive summary

In this paper we present studies related to three magnet families needed for the HL-LHC: (i) the Nb-Ti option for the inner triplet magnets MQXC, which has been developed by CERN in the framework of the sLHC project; (ii) the design of the large aperture two-in-one quadrupole Q4, developed by CEA, and (iii) the actions needed to improve the radiation resistance of resistive magnet in the collimator insertion regions.

1. INTRODUCTION

This report addresses three different magnet families that are needed for the HL-LHC. The first part is devoted to the Nb-Ti option for the inner triplet. This 120 mm aperture quadrupole, named MQXC, was developed since 2007 in the framework of the sLHC project. Here we consider this magnet as an option of the HL-LHC, analysing the consistency of the original choices, made in for a different project, with the HL-LHC targets. The MQXC quadrupole is based on a two layer Nb-Ti coil using the cable of the LHC main dipoles. Two short models were built and tested in the past years. This magnet also made use of a novel insulation scheme allowing a more efficient removal of the heat. The main results are presented both in terms of quench performance and field quality.

The second part of the report is devoted to the design of the Q4 magnet in HL-LHC. In the LHC this magnet has two 70 mm diameter apertures, and is based on Nb-Ti conductor at 4.2 K. It provides 160 T/m operational gradient, with a 3.4 m length. The larger beam size in HL-LHC requires a larger aperture of 90 mm, keeping the same beam interdistance. CEA-Saclay developed in the past three years a design study for this magnet, and the engineering is now in progress. Here we summarize the main design choices: (i) have a 1.9 K operational temperature, (ii) keep an operational point at 80% of the loadline, (iii) use a one layer coil with a LHC dipole cable, leading to small inductance and protection based only on energy extraction.

In the third part of the report we consider the resistive magnets (dipole and quadrupoles) used in the 3 and 7 insertion regions, where the beam cleaning is done through collimators. These magnets should be operational during the whole HL-LHC lifetime, i.e. they should withstand the increased radiation due to highest peak luminosity. The analysis showing the level of radiation in the HL-LHC era is shown, and actions to reduce the radiation dose on the magnet coils are presented. They consist of adding shielding with dense material between the coil and the beam pipe.

2. THE NB-TI OPTION FOR THE INNER TRIPLET

2.1. INTRODUCTION

The High Luminosity LHC (HL- LHC) relies on the Nb_3Sn technology for the inner triplet quadrupoles, in order to maximize the performance in terms of peak luminosity. Since this technology has never been used in accelerators, we also considered a less performing plan B option relying on the Nb-Ti technology. A 120-mm-aperture quadrupole called MQXC has been originally developed for the phase–I upgrade [1,2], to operate in a regime of 2×10^{34} cm^{-2} s^{-1} peak luminosity and to withstand a radiation dose corresponding to 700 fb^{-1}. Here we review the MQXC program in view of the new targets for HL-LHC, namely 5×10^{34} cm^{-2} s^{-1} peak luminosity and 3000 fb^{-1} integrated luminosity. Two short models have been build [3] and tested; we review the performance of these magnets, comparing to the requirements set for HL-LHC.

2.2. OPERATIONAL CONDITIONS: HEAT LOAD AND RADIATION DAMAGE

The option based on the MQXC will have to rely on a thick shielding to limit both heat load and radiation damage. In the HL-LHC baseline, featuring 150-mm-aperture Nb_3Sn triplet, a 6-16 mm-thick tungsten shielding (for Q1 and Q2/Q3 respectively) with a 4-mm-thick stainless steel cold bore and a 2-mm-thick beam screen are enough to reduce the peak heat load below 2 mW/cm^3, and the peak radiation dose below 30 MGy (see Fig. 1 [4]). Note that heat and radiation loads are strongly depending on the angular and longitudinal positions, i.e., these peaks are achieved in localized coil areas.

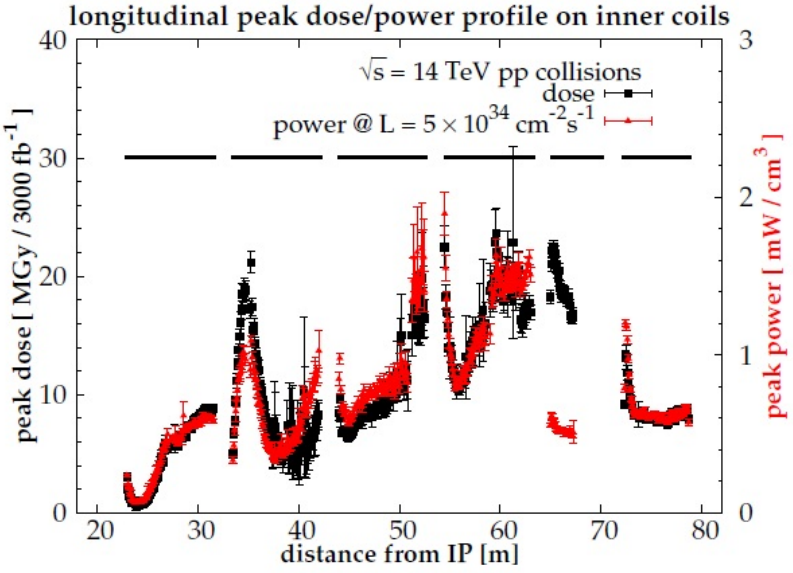

Fig. 1 Heat load and radiation dose for the 150-mm-aperture Nb_3Sn baseline with shielding

For the MQXC option we should envisage a similar thick shielding. We do not have simulations of the energy deposition with the actual MQXC optics, but at first order we can

consider similar loads as in the Nb_3Sn baseline. Therefore we can assume similar targets, i.e. 30 MGy and 2 mW/cm^3. Note that these values are close to what we have for the LHC baseline, thanks to the larger shielding. The consequent reduction in performance has to be evaluated, at first order one can guess the minimal β* between 25 and 40 cm.

To conclude, the MQXC option will need a beam screen shielding that brings the expected heat load and radiation dose to values which are similar or lower to the LHC baseline.

2.3. OPERATIONAL MARGIN

The first estimates of the operational gradient of the MQXC for the phase I was 118 T/m [2], corresponding to operational values at 80% on the loadline (i.e. 20% margin). The gradient has been successively increased up to 123 T/m [5], and then to 127 T/m [6]. For the HL-LHC project we want to keep the original 20% margin, so we set at 118 T/m the operational gradient.

2.4. RESULTS OF THE FIRST TWO SHORT MODELS

Two short models were assembled and tested at CERN in 2012 and 2013 [3]. Results are shown in Fig. 2. Both models have reached nominal gradient of 118 T/m after five quenches. One of them, tested after thermal cycle, reached nominal with one quench. None has been pushed to 90% of short sample, i.e. to 135 T/m (see Fig. 2).

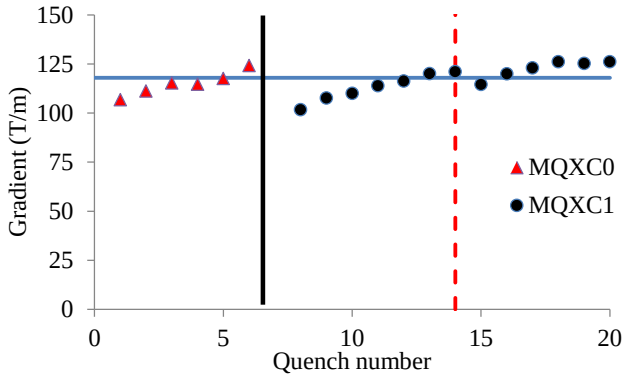

Fig. 2 Training of short models MQXC0 and MQXC1 (red dotted line: thermal cycle)

The performance of these models is not far from the requirements

- A few quenches to nominal in virgin condition (reached)
- At most one quench to nominal after thermal cycle (reached)
- Ability of reaching 90% of short sample in stable conditions (not tried).

On the other hand, the above training indicates that the 20% margin is a reasonable design choice, and it is not wise to reduce it.

2.5. ASSEMBLY FEATURES

The MQXC was originally conceived to be assembled horizontally, and so it was for all components (collars, etc.). In a rather early stage of the project it has been decided to go for a vertical assembly to speed up (see Fig. 3). Vertical collaring cannot be used for assembling

10-m-long magnets, for the lack of an adequate vertical space (10-m-deep shaft plus 10-m-high building). Therefore for full length magnets one should adopt horizontal collaring.

Fig. 3 MQXC assembly: coils around the mandrel (left), the collars around the coils, ground insulation and coil protection sheet (centre) and horizontal collaring (right).

2.6. COIL INSULATION

MQXC features the coil with the enhanced insulation as proposed in [7], where microchannels allow a direct path of the HeII to the strands. The coil modulus with this new insulation is rather close to the LHC dipole coils at the operational pressures of 20-100 MPa. On the other hand, the coil is spongier than the LHC dipole coils and has a large change in dimension (or the order of mm) in the initial phase of assembly, with 0-5 MPa pressures. This makes the assembly more difficult due to larger movements of the components.

The novel insulation scheme ensures a large heat removal, possibly a factor 3 then the LHC dipoles, and first experimental results confirm this feature. Indeed, due to the large shielding, the heat loads will be similar to the LHC baseline, i.e. the novel insulation is not strictly needed. Therefore one should adopt it only if one can prove that this scheme is not increasing risks in assembly and performance. A third MQXC built with the standard insulation would add relevant information for the project.

MQXC adopts a second novel feature, i.e. a ground insulation and collaring shoe which does not seal the coil w.r.t. the collars but with openings to allow HeII to circulate from the coil to the collars and viceversa.

2.7. FIELD QUALITY

This magnet becomes very relevant from the point of view of field quality only at high field, after squeeze. Therefore the field quality requirements are stringent only at 7 TeV, and much less at injection energy. The saturation of the transfer function, i.e. the loss in the strength w.r.t. the linear approximation is expected to be of the order of 70 units (0.7%). This value should pose no problems for operation. The most critical part of field quality is the control of the not allowed harmonics of order 3 and 4.

Measurements of the second model MQXC02 show that one has strong non allowed components b_3 and a_4, of the order of -3 units, i.e. 4 to 5 times the expected standard deviation over a production (see Table 1). This corresponds to a random component which is ~3 times worse than target. These components are not acceptable and should be corrected through a shimming.

There are about 7 units of persistent current in b_6 as expected. The geometric b_6 need fine tuning, i.e. about 7 units have to be added. The origin of this effect has been traced back to an additional 0.1 mm between coil and midplane due to the presence of heaters, not included in the magnetic design phase. Correlations between room temperature and measurements at 1.9 K are good as expected for a self-standing collar structure (see Fig. 4).

Table 1: Measured field harmonics of MQXC02 at 1.9 K, and comparison with target sigma

MQXC02	normal			skew		
	820 A	5000 A +/-	12800 A	820 A	5000 A +/-	12800 A
3	**-3.41**	**-3.56**	**-3.66**	-1.62	-1.78	-2.03
4	0.38	0.66	0.80	**-3.62**	**-3.29**	**-3.05**
5	1.23	0.98	0.88	1.17	0.88	1.15
6	-14.70	-7.99	-7.29	0.69	0.64	0.71
7	-0.35	-0.45	-0.47	-0.70	-0.60	-0.57
8	-0.20	-0.06	-0.02	0.00	0.16	0.17
9	0.17	0.60	0.04	-0.21	-0.22	-0.22
10	1.25	0.68	0.60	-0.22	-0.12	-0.13
14	-0.30	-0.11	-0.05	-0.01	0.01	0.01

sigma	meas/sigma	
	normal	skew
0.820	-4.5	-2.5
0.570	1.4	-5.4
0.420	2.1	2.7
1.100		0.6
0.190	-2.5	-3.0
0.130	-0.2	1.3
0.070	0.6	-3.1
0.200		-0.7
0.023		0.4

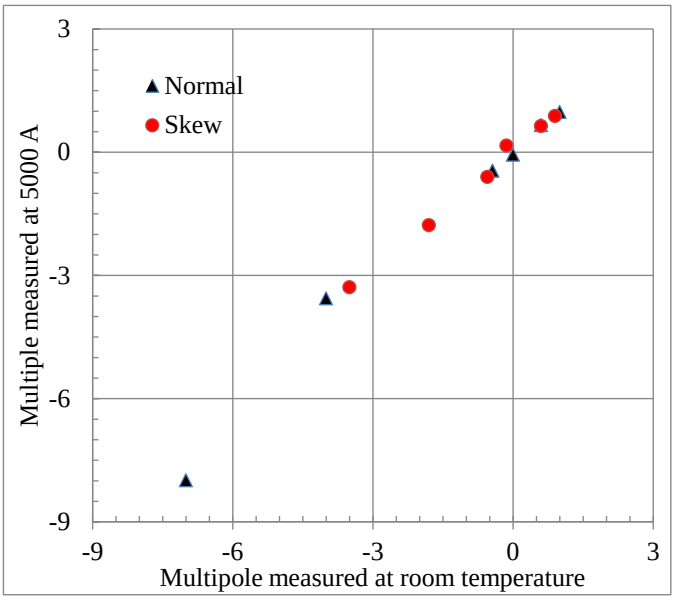

Fig. 4 MQXC02 magnetic measurements [8]: correlations between geometric (average of 5000 A up and down) and room temperature

The magnetic shimming has been successfully proven, showing its ability of correcting a few units of low order not allowed harmonics and a good agreement between the finite element simulations and the magnetic measurements.

2.8. CONCLUSIONS

The MQXC quadrupole, originally thought for the phase-I upgrade, is a viable plan B option for HL-LHC under the condition of having a thick shielding that brings the heat load within

2 mW/cm^3 and the radiation dose below 30 MGy. An estimate of the impact on performance has to be done, the reachable β* being in the range 25-40 cm. We advise to have not less than a 20% loadline margin, corresponding to an operational gradient of 118 T/m. The construction of two short models has shown that this is a reachable target.

Two main open issues have to be decided

- The use of the enhanced insulation, which is not strictly necessary, but that could add operational margin if one can prove that the associated risks are negligible.
- The assembly procedure should be adapted to horizontal assembly and collaring as it was though in the original stage of the project.

Field quality showed that for the model MQXC02 random components are worse than target. It is difficult to judge whether the estimate the random component on the ground of one model is significant. Anyway, this amount of random component can be cured through magnetic shimming, which has been successfully demonstrated for MQXC02.

3. STUDY OF TWO-IN-ONE QUADRUPOLE FOR THE OUTER TRIPLET

3.1. INTRODUCTION

The luminosity upgrade of the Large Hadron Collider aims at gathering 3000 fb^{-1} integrated luminosity [9]. An essential ingredient of the upgrade is the capability of halving the beam size in the interaction point w.r.t. to the LHC baseline: this allows to have denser proton bunches in collision and to increase the peak luminosity. The smaller beam size in the IP corresponds to a larger size in the triplet and in the matching section. For this reason the keyword of the LHC luminosity upgrade is larger aperture magnets [10]. A layout has been proposed, the conceptual design for most magnets has been completed, and first hardware will be tested in 2015.

For the inner triplet (Q1-Q3), the aperture will be increased from the present 70 mm to 150 mm, and will rely on Nb_3Sn technology [11]. For the first quadrupole of the matching section (Q4), called also outer triplet, the aperture will be increased from 70 to 90 mm. Here we outline the conceptual design that has been carried out in the past two years by the CEA-Saclay CERN collaboration [12] for the Q4 magnet.

3.2. REQUIREMENTS AND CONSTRAINTS

Beam dynamics requirements are a 90 mm aperture and a 440 T integrated gradient [13]: this corresponds to a ~30% aperture increase from the Q4 present value of 70 mm aperture, and a ~20% reduction in the integrated gradient (it was 544 T in the LHC [14]). The main constraint in the cross-section is given by the 194 mm beam distance, which will result in a magnetic coupling between the apertures. On the other hand, there are no strong limitations in the longitudinal direction, i.e., one there is flexibility to afford a gradient reduction via a longer magnetic length.

The present Q4 is a 3.4 m-long magnet providing 160 T/m over a 70 mm aperture, relying on Nb-Ti cooled at 4.5 K [14]. For the HL-LHC we plan to use 1.9 K cooling. This allows to have an operational gradient of 115 T/m in a 90 mm aperture, with a 20% margin on the loadline, and a magnetic length of ~3.8 m.

The magnet has two independently powered apertures; the quadrupole is focusing for beam 1 and defocusing for beam 2: this means that both apertures have the same polarity, (as the beams travel in opposite directions). The magnet shall operate in a regime with a current unbalance between apertures up to 50%.

The magnet field quality is critical in collision, i.e. when the main dipoles are powered to bend a 7 TeV beam. Requirements are looser (of the order of 10 units) at injection energy, and tighter (of the order of one unit) at full field. Indeed, in collision the magnet operates in a range of 60-80% of nominal current, so field quality needs optimization over a large range of currents.

Aspects related to cooling and radiation damage are not critical. According to simulations [15], the collision debris induce a heat load of ~6 W on the whole magnet at the nominal peak luminosity of 5×10^{34} cm^{-2} s^{-1}. The cooling system shall be able to remove a static heat load of 50% more, i.e. 9 W. At nominal luminosity, the peak heat load is 0.3 mW/cm^3, which is more than a factor ten below the quench limit established for the LHC magnets in Nb-Ti at 1.9 K. Notwithstanding the comfortable margin, we plan to use an enhanced insulation allowing helium penetration in the strands [7]. Finally, the peak dose for the 3000 fb^{-1} target of HL-LHC integrated luminosity is ~8 MGy. All components are expected to resist to 25 MGy, so also in this case we have a comfortable margin.

3.3. DESIGN OPTIONS

The main issue in the design of the novel Q4 is the coupling between the apertures. Having 97 mm from the beam to the magnet center, and 45 mm of aperture radius, one is left with only 52 mm for the coil, collars and yoke. We choose a simple mechanical structure based on free standing collars, which avoids mechanical coupling between the apertures and the yoke; for this option one needs ~25 mm thick collars. With a 15 mm coil width, only a few mm are left for the iron to magnetically separate the apertures. This constraint excludes the possibility of using a coil width larger than 20 mm (see Fig. 5).

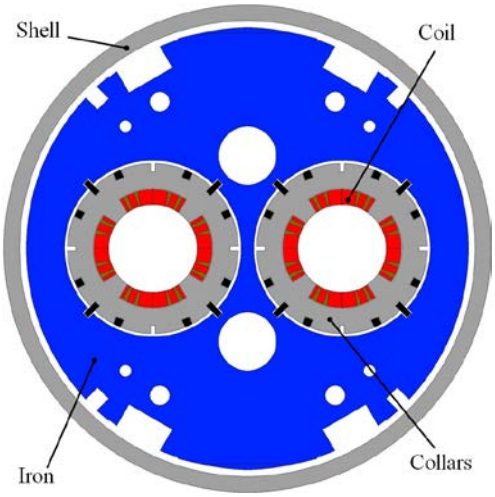

Fig. 5 Cross-section of the large aperture quadrupole Q4

We considered three design options making use of existing Nb-Ti cables: (a) one layer of LHC MQ cable (15 mm width), (b) two layers of LHC MQM cable (8.8 mm width) and (c)

one layer of LHC MQM cable. In all cases we choose a 20% margin on the loadline. Coil cross-sections are shown in Fig. 6 and operational gradients and currents are given in Table 2. Option (a) and (b) have a similar gradient of ~120 T/m, whereas option (c) has 20% less gradient, i.e. about 1 m longer length.

Option (a) presents the advantage of having the cable already available as a spare of the LHC production. Moreover, the short length required (~120 m) allows reusing shorter cuts produced for the LHC that were not usable for the dipoles, which is cost effective. The second advantage is that the large current allows to have shorter time constant in the circuit, and to protect the magnet without quench heaters. These aspects will be discussed in detail in Section 3.7. These advantages of the MQ cable are paid at the price of a larger operational current (16 kA vs 5-7 kA). The final choice has been to use Option (a). The detail of the coil blocks with field maps are shown in Fig. 7.

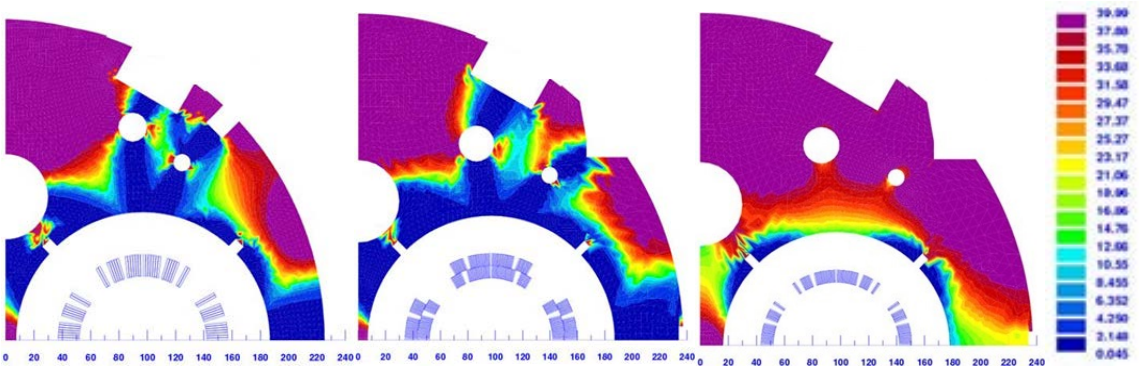

Fig. 6 Three options for the design of the Q4: single layer MQ cable (left), double layer MQM cable (center) and single layer MQM cable (right). Same color scale is used for the permeability in the iron

Table 2: Three options for the Q4 design, with 1.9 K operational temperature

Design option		a	b	c
Cable type		LHC MQ	LHC MQM	LHC MQM
Cable width	(mm)	15.1	8.8	8.8
Layers		1	2	1
Margin	(%)	20	20	20
Current	(kA)	15.65	4.66	6.75
Overall current density	(A/mm^2)	573	520	753
Strand current density	(A/mm^2)	813	763	1104
Gradient	(T/m)	115	123	98
Length	(m)	3.83	3.59	4.50
Stored energy (both ap.)	(MJ/m)	0.190	0.229	0.112
Stored energy (both ap.)	(MJ)	0.73	0.82	0.50
Strand energy density	(J/mm^3)	0.088	0.096	0.100
Inductance per unit length	(mH/m)	0.77	10.14	2.45
Inductance per aperture	(mH)	2.9	36.4	11.0
Dump resistor	(mΩ)	32	107	74
Time constant	(s)	0.09	0.34	0.15

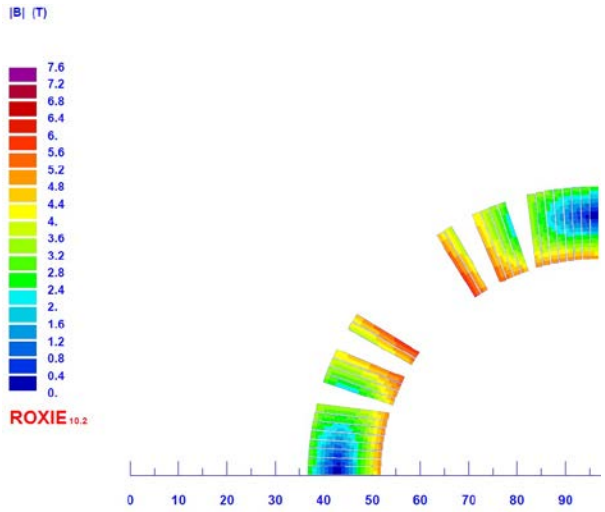

Fig.7 Field in the coil for the option with a single layer MQ cable. Peak field is 6.0 T

3.4. MAGNETIC DESIGN

We now focus on the magnetic design with one layer of the LHC main cable. A three block lay-out with 14 turns allows to optimize field quality, reducing the components b_6, b_{10} to less than one unit, and with 1.5 units of b_{14}, where the reference radius is set at 1/3 of the aperture (see Table 3). At injection there is a non-negligible (~10 units) contribution of persistent currents, which is not critical and therefore is left uncorrected. On the other hand, the geometric b_6 is used to compensate the 0.4 units induced by iron saturation at high field.

On the midplane, an additional insulation of 0.075 mm is placed on each coil, plus a common shim of 0.125 mm. This brings the distance of the first insulated cable to the midplane to 0.1375 mm. The additional midplane is used to allow a tuning of field quality. A change of 0.125 mm in the midplane shim (which corresponds to removing it or doubling) allows correcting b_6 by ±4 units, which is deemed to be enough to fine tune b_6 after the first short model.

Random components of field errors are estimated assuming a random positioning error in the block with 0.025 mm standard deviation for the non-allowed multipoles, and 0.1 mm for the allowed (see Fig. 8). This method has been worked out on the ground of the analysis of the production of several types of quadrupoles based on standard insulation [16].

Table 3: Field Quality Estimate. Allowed multipoles at R_{ref}=30 mm

	Geometric	Saturation	Persistent	Injection	High field
b_6	-0.45	0.40	-11.00	-11.45	-0.05
b_{10}	0.00	0.00	1.00	1.00	0.00
b_{14}	1.50	0.00	0.00	1.50	1.50

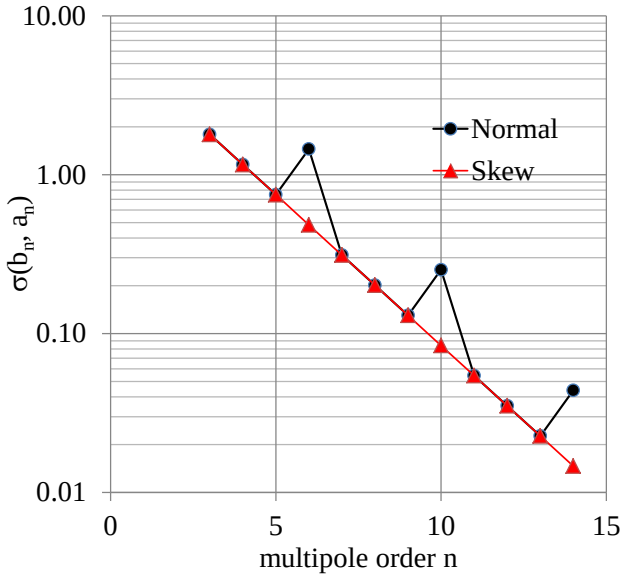

Fig. 8 Estimated random components of multipoles

3.5. MECHANICAL DESIGN

At the nominal gradient of 115 T/m, the accumulation of the Lorentz forces in the magnet midplane induces a stress of the order of 40 MPa. The mechanical structure is the same of the LHC main quadrupole MQ, i.e. self-standing collars. Due to symmetries, the 2D mechanical finite element model, made with CAST3M [17], is restricted to one octant of a single quadrupole magnet cross-section (see Fig. 9). The model includes the front and back collars which simulate the 3D-effect of the stacking in alternated layers. Both elastic and plastic behaviour of the collars and of the keys has been taken into account for the calculation. The other components have been considered with an elastic behaviour. All materials are assumed to be isotropic. Coil modulus is 10 GPa at room temperature, and 15 GPa at 1.9 K, as measured at 50 MPa compression. Integrated thermal contraction of the coil is assumed to be 0.0049.

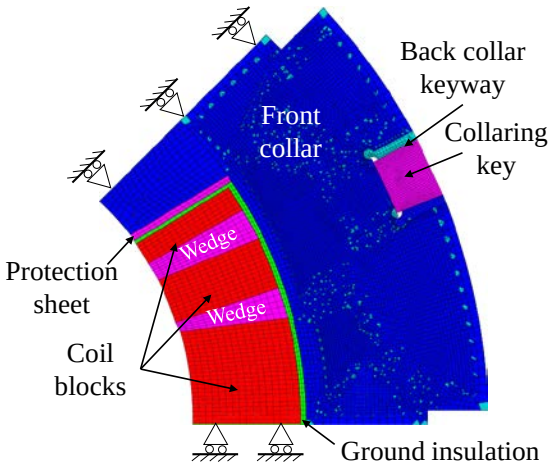

Fig. 9 Mechanical model (one eight of aperture)

The mechanical loading is divided into four phases: collaring process with keys, relaxation due to insulation creep, cool down from 300 K to 2 K and magnetic forces induced by powering up to 110 % of the nominal current. The horizontal and vertical sums of the magnetic forces in one coil octant are then $F_x = 0.44$ MN/m and $F_y = -0.61$ MN/m, respectively. The azimuthal stress distribution obtained in the coil blocks at each phase is presented in Fig. 10. The pre-stress in coil i.e. the average azimuthal stress in coil obtained just after the collaring process with keys is about 80 MPa. A large pre-stress loss due to creep (30%) is assumed [18]. All parts of coils remain in compression at 110 % of the nominal current with a minimum of 10 MPa on the polar plane. Peak stress in coil is below 150 MPa during each loading step and the coil radial displacement due to magnetic forces during excitation is below 50 µm. Therefore, the mechanical studies have validated the magnetic design and the use of free-standing collars as mechanical structure

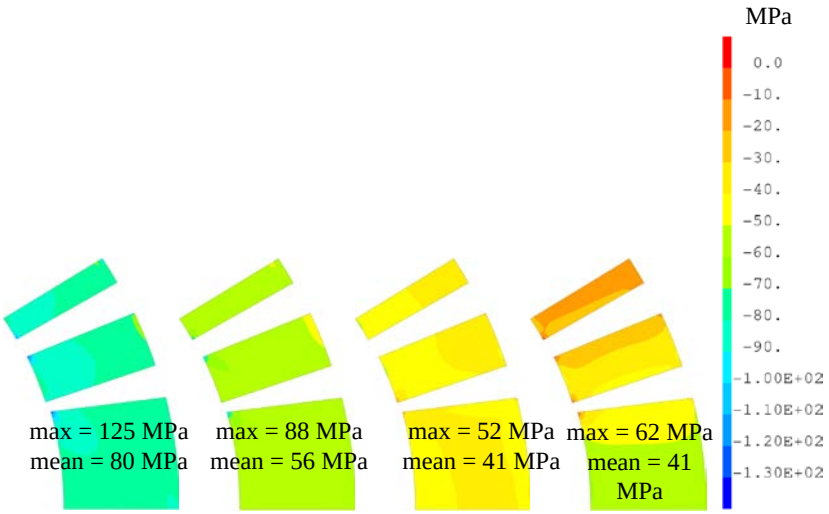

Fig. 10 Azimuthal stress distribution in the coil blocks at each main step: from left to right: collaring with keys, insulation creep, cool down and energisation

3.6. COIL ENDS

The coil ends have been optimized by minimizing both the strain energy of the cable and the peak field. 3D calculations have been realized with ROXIE [19] with a 600-mm-length (straight part + ends) numerical model (see Fig. 11).

As the magnetic design is made of only one layer of MQ cable, the 3D model includes the cable coming from the first winding turn and going out for a connection between coils. This connection cable needs to be in the horizontal position above and along the coil lead-end due to the constraint imposed by the use of free-standing collars as mechanical structure. The coil ends and especially the connection cable have a strong impact on the field quality. Fig. 12 shows the evolution of the pseudo-multipoles b_6 and b_{10} along the 600-mm-long magnet.

The average value of b_6 and b_{10} over this section is 6 units and -1.3 units, respectively. The magnetic design has been adjusted to minimize b_6 and b_{10} when the magnet has the nominal length of 3.8 m. Coil heads also give a systematic b_1 of –8 units and a systematic a_2 of 6 units, both negligible w.r.t. alignment errors. All other terms are below one unit.

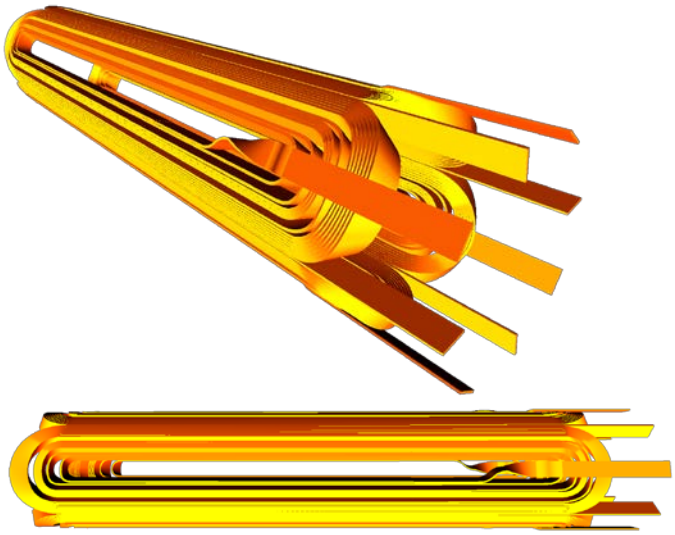

Fig. 11 3D design of the 600-mm-long magnet

The coil ends are long enough to limit as possible the peak field, which is localized in the first conductor of the return end nearby the polar plane of the coil. The coil ends experience a peak field of B_{max} = 6.1 T, 1.5% larger than the 2D calculation (6.0 T).

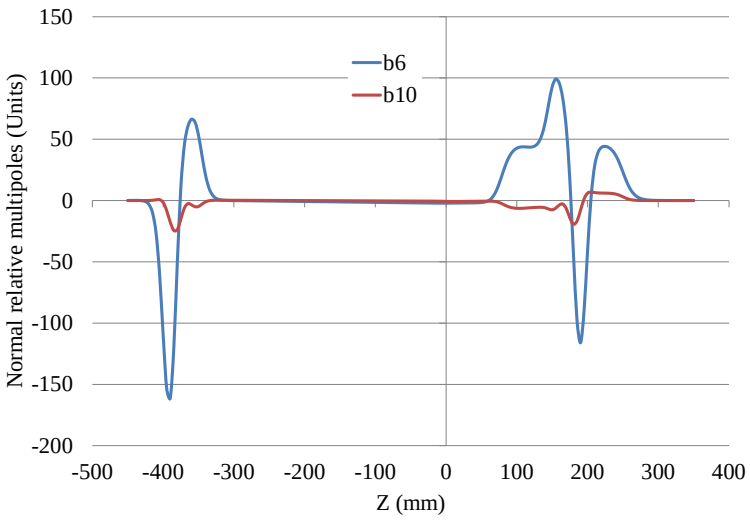

Fig. 12 Evolution of pseudo-multipoles b_6 and b_{10} along the 600-mm-long numerical model

3.7. PROTECTION

In this part, a first evaluation of the magnet protection is given. Computations are performed with the 3D-QTRANSIT code [20] for the operating current and in order to check two criterions: a maximum hot spot temperature of 250 K and a maximum voltage to ground of 500 V. Four different configurations have been studied: no protection, protection with quench heaters only, protection with a dump resistor only and protection with both a dump resistor

and quench heaters. The voltage and detection time of the quench are assumed to be 0.1 V and 10 ms, respectively. The dump resistor is calculated for a maximum voltage to ground of 500 V, corresponding to 32 mΩ. Time of activation (detection time plus heating time) of the quench heaters is supposed to be 40 ms. It is also assumed that a quench appears in the first conductor of the coil near to the polar plane and then it begins to propagate. The evolution of the maximum temperature in quenched coils versus time in the four configurations is obtained (see Fig. 13). In any configurations, the maximum voltage to ground of 500 V is not exceeded.

If the magnet is not protected, the maximum temperature in coil reaches 330 K, which appears too risky. The use of a dump resistor is as efficient as the use of quench-heaters, giving a hotspot temperature in the coil of about 140 K in both cases. Both techniques bring further down the hotspot temperature to 100 K. The simplest option looks the energy extraction on a dump resistor and no quench heaters, which is assumed as a baseline.

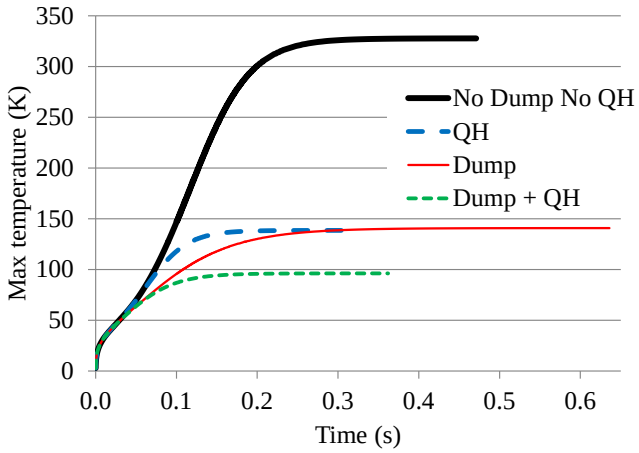

Fig. 13 Evolution of the hotspot temperature in quenched coil versus time in four configurations

3.8. CONCLUSION

In the era of high luminosity LHC, the present 70 mm aperture two-in-one quadrupole Q4 will be replaced by a 90 mm aperture magnet to allow to further squeeze the beams in the interaction point. Here we give the main choices taken for the design of this magnet, based on a Nb-Ti Rutherford cable. The main issue in this design is the coupling between the two apertures. We choose a self-standing collar structure, allowing to decouple the mechanical aspects, and a rather thin (15-mm-width) coil to leave some space to the iron to provide magnetic decoupling. Keeping a 20% margin on the loadline, the operational gradient is 115 T/m. We opted to use a high current cable (LHC main quadrupole) wound in one layer; this choice allows to reuse short lengths of the LHC production that could not be used in the main magnets. Moreover, the large current allows to extract most of the energy on a dump resistor, and to avoid quench heaters thus simplifying the design. The magnetic and mechanical analyses are presented, together with the design of the coil heads. A short model will be built by the CEA-CERN collaboration in 2015-2016.

4. ANALYSIS OF POSSIBLE OPTIONS FOR RESISTIVE QUADRUPOLES AND DIPOLE IN CLEANING INSERTIONS

4.1. INTRODUCTION

MQW and MBW are normal conducting magnets, presently used in the LHC IP 3 and IP 7 (cleaning insertion areas). The coils are insulated with glass fibres tapes (type E) and impregnated with epoxy resin. It is known that epoxy, as any other organic insulator, will degrade in function of the accumulated ionizing radiation dose. The motivations of the described interventions are:

- To insure that the set of installed magnets will survive till Long Shutdown 3 (LS3 integrated luminosity 350 fb^{-1}), increasing LHC reliability
- As these magnets do not need upgrade to fit the HL-LHC optics, the aim is to increase as much as possible their lifetime in the HL-LHC era (till 3000 fb^{-1})

The proposed program takes into account the following criteria

- Minimization of the dose absorbed by the operators (ALARA) by means of anticipation of interventions. This allow reducing the radiation cooling time and dose rate emitted by the equipment will be much lower respect to later stage intervention.
- Reduction of risk of failure during the HL-LHC Physics run
- Reduction of capital cost investment (reduction of investment to build new magnets)
- Optimised management of the spares (keep non active spare as long as possible)

4.2. TECHNICAL ANALYSIS

4.2.1. Epoxy recipe used for vacuum impregnation during fabrication of coils.

The two magnet types feature very different epoxy system leading to different radiation resistance (See Table 4).

Table 4: Recipe of resin compound used for the vacuum coil impregnation. Factor K - quantity of epoxy groups in a resin on an elemental composition. Quantity in part per weight (ppw)

	MQW	MBW
Resin 1 (ppw)	EPN1138 (50 ppw)	D-16 (100 ppw)
Resin 2 (ppw)	GY 6004 (50 ppw)	-
Resin 3 (ppw)	CY 221 (20 ppw)	-
Hardener (ppw)	HY 905 (120 ppw)	MA 2.28 × K
Accelerator (ppw)	DY 073 (0.3)	TEA

4.2.2. Filler/reinforcement in the insulation system

Both magnet types have glass tapes as filler (see Table 5).

Table 5: Filler and insulation layer compositions

	MQW	MBW
Inter turn	2×(2×0.25) mm=1 mm glass tape	2×(2×0.15)=0.6 mm glass tape
Inter layer	No layers	2×(2×0.15)+2×(2×0.15)+1(glass cloth) =1.6 mm glass tape
To ground	1×(2×0.25) mm+3X(2×0.25)= 2 mm glass tape	2×(2×0.15)+1.5(0.15×6=1.8 mm glass tape

4.2.3. Estimation of insulation stresses

According to FLUKA estimation, the most exposed area in the MQW magnet is the start of the coils along the straight part. A 2D Ansys™ model coupling magnetic and mechanical analysis has been built providing the following results for a current of 710 A.

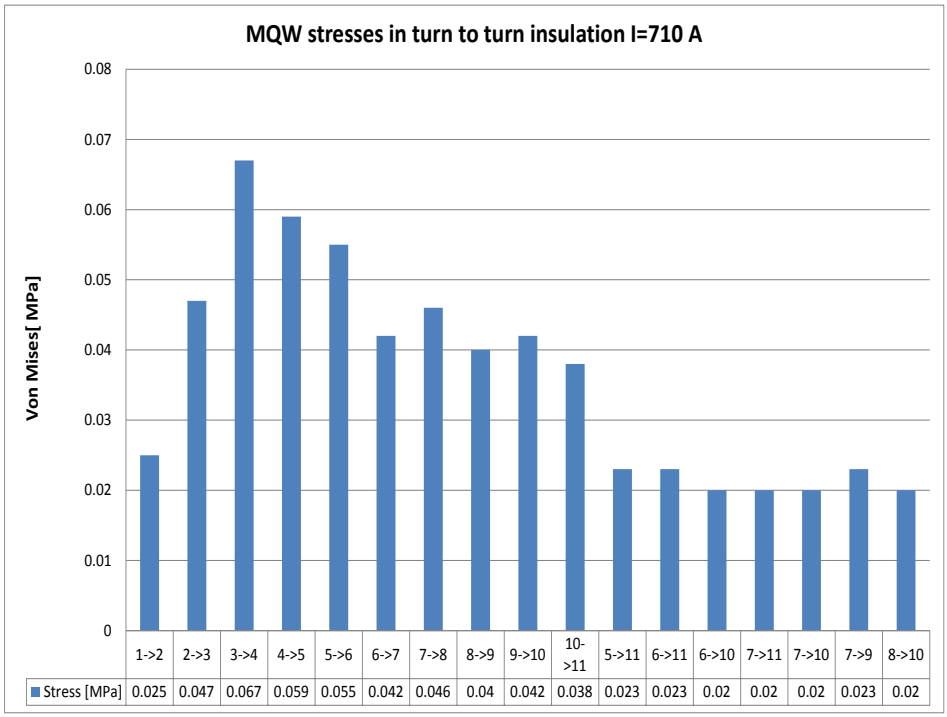

Fig. 14 Stress intensity factor insulation between conductors

The computed stresses are always lower than 1 MPa. As consequence a reference values for which the resin shall demonstrate to be still operational is set at **10 MPa**. This takes into account that measurement for values lower then 2-3 MPa are meaningless and it provides safety margin.

For MBW similar computations have not been performed yet, but on the base of the previous ones the threshold of 10 MPa is assumed and it shall be considered to be a conservative choice. In this case the critical spot is on the coil front end and not in the magnet straight part.

4.2.4. Estimation of resin radiation resistance

Using the available experimental data [21,22,23,24] on the two resins compound and scaling them taking into account the enhancement from the fillers it is possible to build the following indicative table:

Table 6: Estimation of level of damage for MQW and MBW insulation system

Magnet	Limited aging, pure resin would stand		Aging, range achievable thanks to filler		Start of failure
	Min [MGy]	Max [MGy]	Min [MGy]	Max [MGy]	From [MGy]
MQW	10	20	20	50	50
MBW	40	60	60	80	80

The MQW design presents also a spacer to keep in place the coils during energization. This spacer (or shim) is made of High Density Polyethylene pipes filled with epoxy resin cured at room temperature.
Here the details of the system according to the recipe provided by the manufacturing drawing (quantity to be prepared for 1 magnet)

1) Resin: EPON 826, 22 kg, low viscosity bisphenol A epoxy resin
2) Hardener, RP 1500, 3 kg, tetramine hardener
3) Filler MIN-SIL 120 F, 17 kg, Fused silica particles 50% diameter smaller than 0.044 mm

The component is submitted to stresses of the order or less than 0.1 MPa and the usual value of 10 MPa is assumed here as reference limit after irradiation.
Similar composition material (Araldite D) presents a radiation limit of about 10 MGy [21,22,23]. Filler should increase lifetime till at least 20 MGy. This is the limit that is assumed. For such capability to stand radiation it is necessary, according to FLUKA computations, to have a shielding also on these components.

4.2.5. Estimation of doses

In Table 7 the estimated doses following the extensive FLUKA computations are presented.

1) In yellow range of no or limited ageing. Pure resin would stand
2) In orange range achievable thanks to the filler
3) In red where insulation system could start failing. In absence of better measurement or data preventive change of magnet recommended.

Remark for colour level in terms of MGy see chapter on the resin radiation resistance for MBW and MQW.

Table 7: Integrated Dose map for IP3 Left and Right at integrated luminosity of LS2 (150 fb^{-1}), LS3 (350 fb^{-1}) and end of HL-LHC exploitation (3000 fb^{-1}).

	Dose [MGy] for integrated luminosity 150 fb^-1		Dose [MGy] for integrated luminosityy350 fb^-1		Dose [MGy] for integrated luminosity3000 fb^-1	
	R	L	R	L	R	L
MQWA.A4	0.0	0.1	0.1	0.2	1.0	1.9
MQWA.B4	0.1	0.1	0.1	0.2	1.0	2.1
MQWB.4	0.1	0.1	0.1	0.3	1.1	2.2
MQWA.C4	0.1	0.1	0.2	0.3	1.4	2.8
MQWA.D4	0.2	0.3	0.4	0.8	3.5	6.9
MQWA.E4	0.9	1.7	2.0	4.0	17	35
MQWA.A5	0.6	1.1	1.3	2.6	11	22
MQWA.B5	0.7	1.4	1.6	3.2	14	28
MQWB.5	1.7	3.3	3.9	7.7	33	66
MQWA.C5	3.9	7.7	9.0	18	77	155
MQWA.D5	0.9	1.9	2.2	4.3	19	37
MQWA.E5	1.7	3.5	4.0	8.1	35	69
MBW.A6	1.0	2.0	2.3	4.6	20	40
MBW.B6	1.2	2.3	2.7	5.4	23	46
MBW.C6	1.6	3.3	3.8	7.6	33	65

Table 8: Integrated Dose map for IP7 Left and Right at integrated luminosity of LS2 (150 fb^{-1}), LS3 (350 fb^{-1}) and end of HL-LHC exploitation (3000 fb^{-1}).

	Dose [MGy] for integrated luminosity 150 fb^-1		Dose [MGy] for integrated luminosityy350 fb^-1		Dose [MGy] for integrated luminosity3000 fb^-1	
	R	L	R	L	R	L
MQWA.A4	0.4	0.5	0.9	1.2	7.4	11
MQWA.B4	0.3	0.8	0.7	1.9	6.4	16
MQWB.4	0.5	1.3	1.2	2.9	10	25
MQWA.C4	4.0	4.0	9.3	9.3	80	80
MQWA.D4	2.7	2.7	6.2	6.2	53	53
MQWA.E4	5.0	10	12	23	100	199
MQWA.A5	2.6	2.6	6.1	6.1	52	52
MQWA.B5	3.5	3.5	8.1	8.1	69	69
MQWB.5	4.1	4.1	9.5	9.5	81	81
MQWA.C5	1.9	4.9	4.5	11	39	97
MQWA.D5	4.2	6.0	10	14	84	120
MQWA.E5	37	12	86	29	738	246
MBW.A6	23	17	54	39	465	332
MBW.B6	37	19	87	43	745	372

4.3. PROPOSED ACTIONS

4.3.1. Shield installation

The installation of shielding in tungsten alloy is done in order to absorb particles before that they reach the coils. Two different designs have been developed for MBW and MQW being very different the place where the coil had to be screened (MBW: coil heads, MQW coil straight part). In Fig. 16 an example of the reduction of the absorbed dose for the most exposed MQW magnet with the use of the screen on the initial 50 cm of the magnet length. The efficiency on the MBW magnet is similar producing a reduction to 30%. The detail of the shielding is shown in Figs. 17and 18

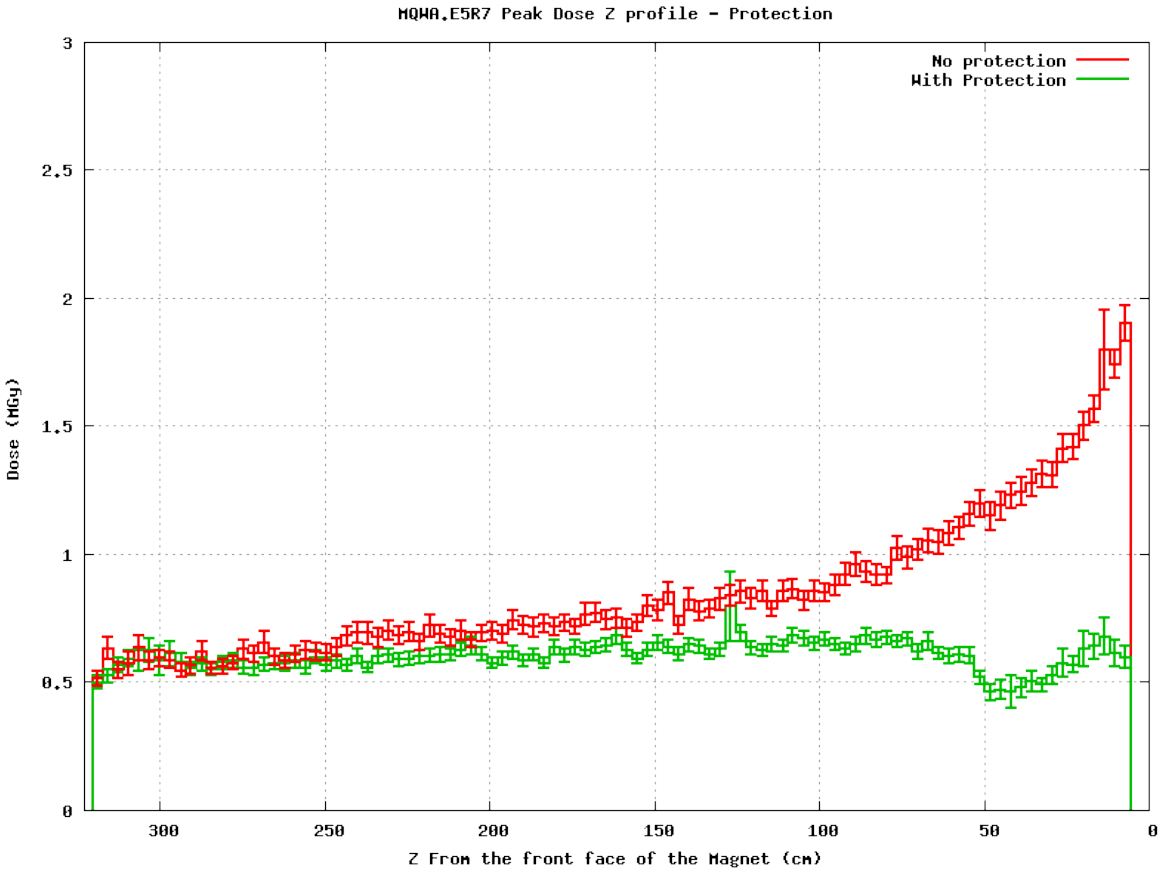

Fig. 16 Effect of 50 cm long coil shield on the most exposed MQW magnet in IP7

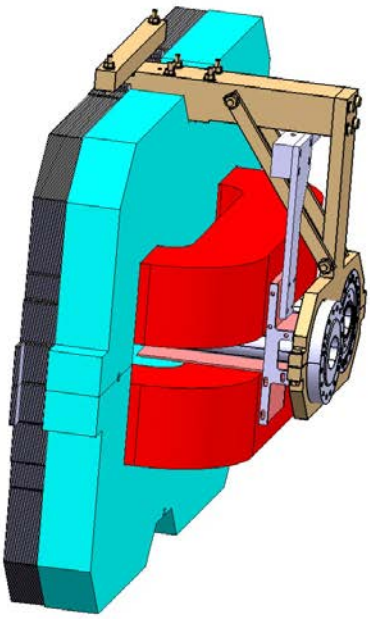

Fig. 17 Installation of the shielding on the MBW magents: coil in red, iron yoke in blue, shielding in pink: protecting the coil on the front face and towards the vacuum chamber.

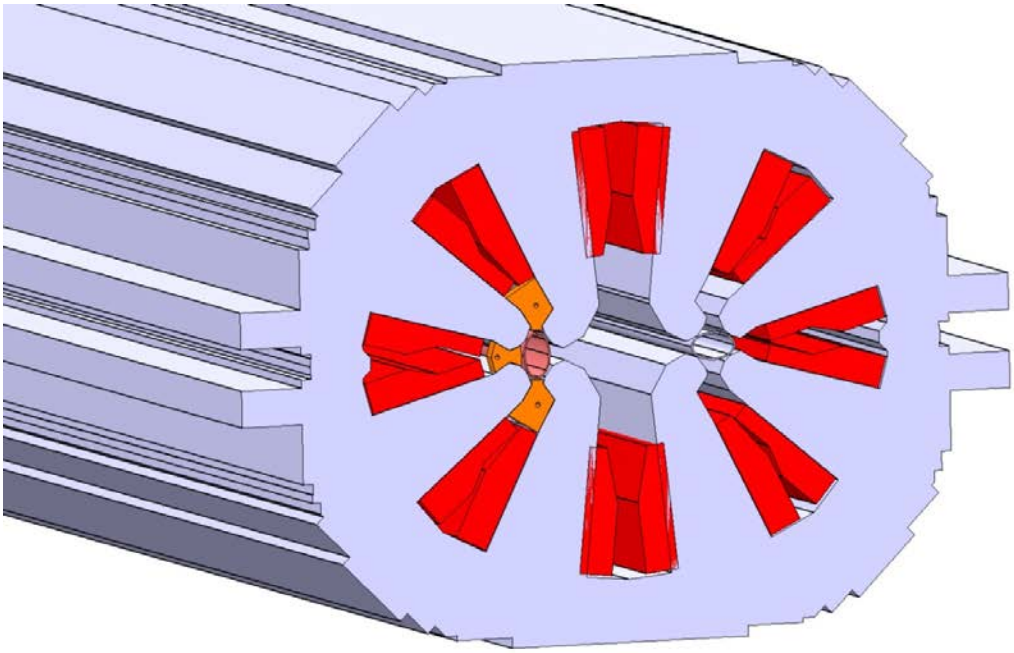

Fig. 18 Installation of the shielding in the MQW magnets straight part: coil in red, iron yoke in grey, shielding in orange: protecting the coil towards the vacuum chamber.

4.3.2. Modification of machine optics

MQW magnets are connected in series of 5 plus an independent powered trim. As the foreseen current at 7TeV for the MQWB trim in IP7 R and L is very small (about 20 A) the following action is under study

1) Reconfigure the MQWB as an MQWA magnet
2) Remove the 1st MQWA magnet of the chain of 5, being the most exposed.
3) Connect in series the previous MQWB (now MQWA) with the other MQWA in cell 5 in other to re-establish the necessary integrated gradient
4) Replace the MQWA removed with an absorber in order to protect the series of MQW quadrupoles.

This action shall be take place in LS2 and it should undergo final validation from the beam optics team.

4.3.3. Magnet replacement

In case applying the previous mentioned actions it would not be possible to guarantee the reliability of the machine, it would be necessary to design and installed magnet resistant to very high radiation dose. For the dipole such magnet should present saddle shape heads, while the quadrupole should use mineral insulators.

Table 9 and 10 present the dose absorbed with the magnet introducing staged shielding approach where the most exposed unit would be shielded in LS1 while the other exposed unit would be shielded in LS2. Tis would allow reducing the absorbed does mitigating the risk of a possible impact of this action of the LHC start up after LS1

Table 9: Magnet doses with tungsten screen in IP3 Right (R) and Left (L)

	Dose [MGy] for integrated luminosity 150 fb^-1		***Dose [MGy] for integrated luminosityy350 fb^-1***		***Dose [MGy] for integrated luminosity3000 fb^-1***	
	R	**L**	**R**	**L**	**R**	**L**
MQWA.A4	0.0	0.1	0.1	0.2	1.0	1.9
MQWA.B4	0.1	0.1	0.1	0.2	1.0	2.1
MQWB.4	0.1	0.1	0.1	0.3	1.1	2.2
MQWA.C4	0.1	0.1	0.2	0.3	1.4	2.8
MQWA.D4	0.2	0.3	0.4	0.8	3.5	6.9
MQWA.E4	0.9	1.7	**1.2**	**2.5**	**6.3**	**11.8**
MQWA.A5	0.6	1.1	**0.8**	**1.6**	**4.0**	**7.5**
MQWA.B5	0.7	1.4	**1.0**	**2.0**	**5.1**	**9.4**
MQWB.5	1.7	3.3	**2.4**	**4.8**	**12.1**	**22.6**
MQWA.C5	3.9	7.7	**5.6**	**11.2**	**28.3**	**52.8**
MQWA.D5	0.9	1.9	**1.3**	**2.7**	**6.8**	**12.7**
MQWA.E5	1.7	3.5	**2.5**	**5.0**	**12.7**	**23.6**
MBW.A6	1.0	2.0	**1.4**	**2.9**	**7.3**	**13.6**
MBW.B6	1.2	2.3	**1.7**	**3.3**	**8.4**	**15.7**
MBW.C6	1.6	3.3	**2.3**	**4.7**	**11.9**	**22.2**

Table 10: Magnet doses with tungsten screen in IP7 Right (R) and Left (L)

	Dose [MGy] for integrated luminosity 150 fb^-1		***Dose [MGy] for integrated luminosityy350 fb^-1***		***Dose [MGy] for integrated luminosity3000 fb^-1***	
	R	**L**	**R**	**L**	**R**	**L**
MQWA.A4	0.4	0.5	0.9	1.2	7.4	10.6
MQWA.B4	0.3	0.8	0.7	1.9	6.4	16.0
MQWB.4	0.5	1.3	1.2	**1.8**	10.1	**9.3**
MQWA.C4	4.0	4.0	**5.8**	**5.8**	**29.3**	**29.3**
MQWA.D4	2.7	2.7	**3.8**	**3.8**	**19.5**	**19.5**
MQWA.E4	5.0	10.0	**7.2**	**14.4**	**36.6**	**73.1**
MQWA.A5	2.6	2.6	**3.7**	**3.7**	**19.0**	**19.0**
MQWA.B5	3.5	3.5	**5.0**	**5.0**	**25.4**	**25.4**
MQWB.5	4.1	4.1	**5.9**	**5.9**	**29.7**	**29.7**
MQWA.C5	1.9	4.9	**2.8**	**7.0**	**14.2**	**35.6**
MQWA.D5	**1.4**	**2.0**	**3.3**	**4.7**	**27.9**	**39.9**
MQWA.E5	**12.3**	**4.1**	**28.7**	**9.6**	**246.0**	**82.0**
MBW.A6	**7.8**	**5.5**	**18.1**	**12.9**	**155.2**	**110.8**
MBW.B6	**12.4**	**6.2**	**29.0**	**14.5**	**248.3**	**124.1**

4.4. CONCLUSION

With the application of the proposed strategy the situation would be the following

1) IP 3:
    a. MQW magnet left of point 3 (L3) would be marginal to reach the HL-LHC full integrated luminosity
    b. MBW not magnet to be changed
2) IP 7:
    a. MQW: 3 magnets would need to be replaced before the HL-LHC era. Of these two (MQWA.E5 in R7 and L7) will be saved with the application of the proposed optic change. For MQWA.E4 in L7 installation of local absorber shall be studied
    b. MBW: 4 magnets (MBW.A6 L and R and MBW.B6 L and R) shall be changed. These units would need to be equipped with coils with saddle heads

REFERENCES

[1] J.P. Koutchouk, L. Rossi, E. Todesco, "A solution for the phase I upgrade based on Nb-Ti", (2007) LHC Project Report 1000.
[2] R. Ostoijc, et al, "Conceptual design of the LHC interaction region upgrade – Phase I" (2008) LHC Project Report 1163.
[3] G. Kirby, et al., "Testing results for Nb-Ti 120-mm-aperture low-beta quadrupooe models for the LHC high luminosity insertion" (2013) MQXC. Submitted to: IEEE Trans. Appl. Supercond. *ASC Conference proceeding*, 2012 Portland, also CERN ATS-2013-041.
[4] L. Esposito, F. Cerutti, E. Todesco, "Fluka energy deposition studies for the HL LHC" (2013) *International Particle Conference2013*, Shanghai, see www.jacow.org .
[5] S. Fartoukh, "Optics challenges and solutions for the LHC insertions upgrade phase I" (2010) *Chamonix 2012 proceedings*, also CERN-ATS-2010-026.
[6] S. Russenschuck, et al., "Design challenges of a wide-aperture insertion quadrupole magnet" (2011) *IEEE Trans. Appl. Supercond.* **21**(2011) 1674-8, also CERN-ATS-2011-084.
[7] D. Tommasini, M. La China, "Cable insulation scheme to improve heat transfer to superfluid helium in Nb-Ti accelerator magnets" (2008) *IEEE Trans. Appl. Supercond.* **18** (2008) 1285-8, also CERN-AT-2008-005.
[8] L. Fiscarelli, "MQXC02 magnetic measurements" presented at magnet group technical meeting, July 2014.
[9] L. Rossi, et al., "High Luminosity Large Hadron Collider: A description for the European Strategy Preparatory group", CERN-ATS-2012-236.
[10] E. Todesco, et al., 'A First Baseline for the Magnets in the High Luminosity LHC Insertion Regions', *IEEE Trans. Appl. Supercond.* **24** (2014).
[11] P. Ferracin, "Magnet design of the 150 mm aperture low-□ quadrupoles for the high luminosity LHC", *IEEE Trans. Appl. Supercond.* **24** (2014).
[12] M. Segreti, J. M. Rifflet, Studies on large aperture Q4 with MQ and MQM cables – I, II and III report", http://www.cern.ch/hilumi/wp3.
[13] R. De Maria, WP2 meeting on June 27th 2014, see web page https://indico.cern.ch/event/323860/
[14] R. Ostojic, "The LHC insertion magnets", *IEEE Trans. Appl. Supercond.* **12** (2002) 196-201.
[15] L.S. Esposito et al. "FLUKA energy deposition studies for the HL-LHC", Proceedings of IPAC2013, TUPFI021 and talk given at WP3 on 22 May 2014, www.cern.ch/hilumi/wp3
[16] B. Bellesia, J. P. Koutchouk, E. Todesco, `Field quality in low-beta superconducting quadrupoles and impact on the beam dynamics for the Large Hadron Collider', *Phys. Rev. STAB* **10** 062401 (2007).
[17] CASTEM. Software for Finite Element Method (FEM) computations. CEA product.
[18] P. Fessia *et al.*, "Electrical and Mechanical Performance of an Enhanced Cable Insulation Scheme for Superconducting Magnets", *IEEE Trans. Appl. Supercond.*, vol. 20, no. 3, pp. 1622–1625, 2010.
[19] S. Russenschuck, "Field computation for accelerator magnets" Wiley VCH, 2011.
[20] 3D-QTRANSIT. Software for simulation of quench propagation in superconductor magnets. CEA product.
[21] Compilation or Radiation Damage Test Data Part II CERN 79-08

[22] Compilation or Radiation Damage Test Data Part II CERN 98-01
[23] Radiation tests of selected electrical insulator materials for high power and high voltage applications CERN 88-02
[24] BINP tests on D16. Private communications

ANNEX: GLOSSARY

Acronym	Definition
LHC	Large Hadron Collider
HL-LHC	High Luminosity LHC
MQXC	120-mm-aperture quadrupole developed for the phas-I upgrade
CAST3M	Finite element code
ROXIE	Software for magnetic modelling of accelerator magnets
Q4	Fourth quadrupole from the IP, after the triplet, separation and recombination dipole
3D-QTRANSIT	Software for quench simulation
IR	Interaction Regions
LARP	LHC Accelerator Research Program
BINP	Budker Institute of Nuclear Physics
LS1	Long Shutdown I taking place in 2013 and 2014
LS2	Long Shutdown II taking place from 1.5 year when the machine will receive an integrated luminosity of 150 fb^{-1}
LS3	Long Shutdown III taking place for 2 years when the machine will receive an integrated luminosity of 350 fb^{-1} . during this shut down the largest number of equipment for the HL-LHC will be installed
R3	Right of point 3
L3	Left of point 3
R7	Right of point 7
L7	Left of point 7